Ning, T., Wickert, J., Deng, Z., Heise, S., Dick, G., Vey, S., Schöne, T. (2016): Homogenized time series of the atmospheric water vapor content obtained from the GNSS reprocessed data. - *Journal of Climate*, *29*, 7, pp. 2443–2456.

DOI: http://doi.org/10.1175/JCLI-D-15-0158.1

Homogenized Time Series of the Atmospheric Water Vapor Content Obtained from the GNSS Reprocessed Data

T. Ning,* J. Wickert, Z. Deng, S. Heise, G. Dick, S. Vey, and T. Schöne

Section 1.1: GPS/Galileo Earth Observation, and Section 1.2: Global Geomonitoring and Gravity Field, GFZ German Research Centre for Geosciences, Potsdam, Germany

(Manuscript received 10 February 2015, in final form 11 January 2016)

ABSTRACT

The potential temporal shifts in the integrated water vapor (IWV) time series obtained from reprocessed data acquired from global navigation satellite systems (GNSS) were comprehensively investigated. A statistical test, the penalized maximal *t* test modified to account for first-order autoregressive noise in time series (PMTred), was used to identify the possible mean shifts (changepoints) in the time series of the difference between the GPS IWV and the IWV obtained from the European Centre for Medium-Range Weather Forecasts (ECMWF) interim reanalysis (ERA-Interim) data. The approach allows for identification of the changepoints not only in the GPS IWV time series but also in ERA-Interim. The IWV difference time series formed for 101 GPS sites were tested, where 47 of them were found to contain in total 62 changepoints. The results indicate that 45 detected changepoints were due to the inconsistencies in the GPS IWV time series, and 16 were related to ERA-Interim, while one point was left unverified. After the correction of the mean shifts for the GPS data, an improved consistency in the IWV trends is evident between nearby sites, while a better agreement is seen between the trends from the GPS and ERA-Interim data on a global scale. In addition, the IWV trends estimated for 47 GPS sites were compared to the corresponding IWV trends obtained from nearby homogenized radiosonde data. The correlation coefficient of the trends increases significantly by 38% after using the homogenized GPS data.

1. Introduction

Water significantly affects Earth's climate system by constantly changing its states (vapor, liquid, and solid) within the hydrospheric cycle, which is regulated by the temperature (Bengtsson 2010). Under the assumption of conserved relative humidity, the relation between the changes in total atmospheric water vapor content and the change in the surface air temperature is represented by a ratio of approximately 7% K^{-1} (Trenberth et al. 2003). Additionally, water vapor is a very efficient greenhouse gas (Buehler et al. 2006). The long-term change in the integrated water vapor (IWV) in the atmosphere is therefore important for climate monitoring.

* Current affiliation: Lantmäteriet (the Swedish Mapping, Cadastre and Land Registration Authority), Gävle, Sweden.

Corresponding author address: T. Ning, Section 1.1: GPS/Galileo Earth Observation, GFZ German Research Centre for Geosciences, Telegrafenberg, 14473 Potsdam, Germany.
E-mail: tongn@gfz-potsdam.de

DOI: 10.1175/JCLI-D-15-0158.1

Based on the path delay of radio signals propagating through Earth's neutral atmosphere, the IWV can be derived from observations acquired from global navigation satellite systems (GNSS) [e.g., the global positioning system (GPS)]. Since GNSS observations acquired from the ground can be made during all weather conditions, with a high temporal resolution (a few minutes), and with a high reliability, the IWV trends estimated from the GNSS data are important for climate applications and are investigated by many studies (e.g., J. Wang et al. 2007; Vey et al. 2010; Ning et al. 2013). Meanwhile, ground-based GNSS IWV was identified as a priority 1 measurement for the Global Climate Observing System (GCOS) Reference Upper-Air Network (GRUAN) as one of the reference data. The objective of the GRUAN is to provide long-term, high-quality upper-air climate records, to constrain/calibrate data from more spatially comprehensive global observing systems (including satellites), and to measure a large suite of correlated climate variables (Seidel et al. 2009).

Realistic and reliable climate signals can only be obtained from homogeneous data. Different changes may take place during the period of the data recording of a GNSS site, and those changes can be either data processing related or site related (Vey et al. 2009).

The data-processing-related changes are due to inconsistencies in GNSS data processing: that is, updates of the reference frame and applied models, different elevation cutoff angle, different mapping functions, and different processing strategies. Steigenberger et al. (2007) found that such changes can cause inconsistencies of several millimeters in the GNSS-derived tropospheric delay time series. They also found that a homogenous data reprocessing over the whole data time series can significantly reduce processing-related inconsistencies.

The site-related changes comprise the replacements of hardware (receivers, cables, antennas, and radomes), the difference in measurements (such as number of visible GNSS satellites and data rate), and the change of the electromagnetic environment, which may cause different effects of signal multipath. The hardware changes and the difference in measurements usually result in a constant offset (Johansson 1998), while the inconsistences due to the latter change are normally varying when reflective properties change. For example, a bias due to growing vegetation changes continuously for a certain time period (Pierdicca et al. 2014), while the cutting of trees and/or different soil moisture (i.e., rain and snow) introduce a sudden bias (Larson et al. 2010). Signal multipath effects are worse for observations at low elevation angles. Therefore, higher elevation cutoff angles are recommended for the IWV trend estimation because the formal error of the IWV is not the limiting factor for this application (Ning and Elgered 2012). The multipath effects can also, to a large extent, be removed by implementing microwave-absorbing material below the GNSS antenna plane (Ning et al. 2011), which however can introduce shifts in the IWV time series after the absorber is implemented. A mean shift of about 0.4 kg m^{-2} was found by Gradinarsky et al. (2002) after a radome change took place at one of the International GNSS Service (IGS) sites, ONSA (57.4°N, 11.9°E). A more systematic study on the homogeneity of globally GPS-derived IWV time series was carried out by Vey et al. (2009), who found that changes of GNSS antennas and radomes, as well as changes in the number of observations, can all cause significant shifts in the IWV time series.

In this work, the possible temporal shifts in the IWV time series obtained from the reprocessed GPS data were investigated. The time series of the IWV difference were first formed between the GPS data and the European Centre for Medium-Range Weather Forecasts (ECMWF) interim reanalysis (ERA-Interim) data. A statistical test was carried out on the formed IWV difference time series in order to detect potential mean shifts (changepoints). In addition, a further validation was performed in order to distinguish the GPS-related changpoints from the ones caused by the ERA-Interim data. In section 2 the details of the reprocessed GPS data and ERA-Interim are described. The penalized maximal t test modified to account for first-order autoregressive noise in time series (PMTred) used for the changepoint detection is introduced in section 3, where the approach used to validate detected changepoints is also discussed. Section 4 presents results both for all detected changepoints and for comparisons of the IWV trends before and after implementing the bias correction to the GPS data. Conclusions are given in section 5.

2. Datasets and analysis procedures

a. GPS data

As one of the IGS Tide Gauge Benchmark Monitoring (TIGA) Analysis Centers (Schöne et al. 2009), the German Research Centre for Geosciences (GFZ) contributed to the IGS TIGA reprocessing campaign where the GPS data acquired from 794 globally distributed sites (see Fig. 1), covering the time period from January 1994 to December 2012, were homogenously reprocessed (Deng et al. 2016). Some details about the data reprocessing are described below:

- Earth's ionosphere contains electrons in sufficient quantity to significantly delay the propagation of GNSS signals. To remove this impact, the ionosphere-free linear combination of the carrier phase measurements was used for the data processing. Together with undifferenced carrier phase and pseudorange observables, the data were processed using GFZ's in-house GNSS software package, Earth Parameter and Orbit Determination System (EPOS) (Deng 2012).
- To obtain the highest accuracy in the ZTD estimates, antenna related errors [i.e., phase center offsets (PCO) and phase center variations (PCV)] need to be reduced. Therefore, calibrations for both satellite and ground antenna PCOs and PCVs were applied (Schmid et al. 2007).
- Although GNSS carrier phase measurements are much more accurate, they are ambiguous by an integer multiple of one cycle. It is therefore important that the value of this ambiguity must be resolved and be fixed at its correct integer value (Teunissen 1995). In our data processing, the ambiguity resolution was applied.
- Ocean tide loading correction was implemented using a finite element solution model (FES2004; Lyard et al. 2006).

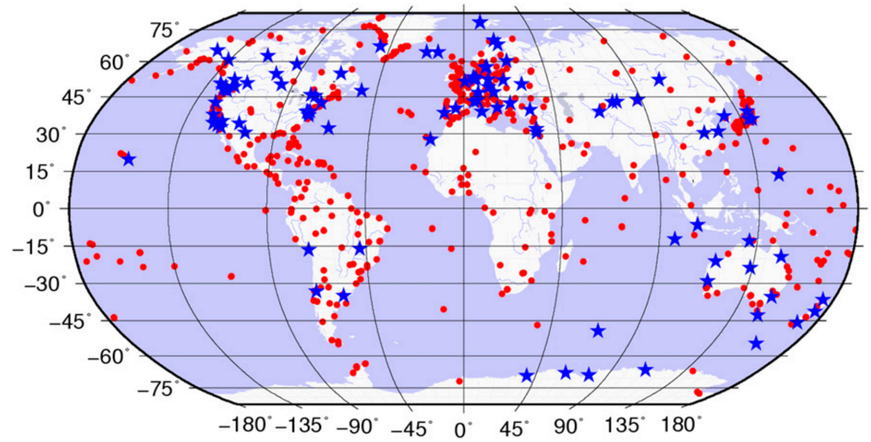

FIG. 1. Geographical location of all GPS sites that were included in the TIGA data reprocessing. Stars indicate the sites with a time series of data longer than 15 yr, which were used for the PMTred test in this work.

- An a priori zenith total delay (ZTD) was first formed by the sum of an a priori zenith hydrostatic delay (ZHD) and an a priori zenith wet delay (ZWD). The a priori of ZHD was obtained using the model presented by Saastamoinen (1973), and a value of 0.1 m for the a priori ZWD was used for all GPS sites. Corrections for the a priori ZTD together with the horizontal delay gradients were estimated using the Vienna mapping function 1 (VMF1) (Böhm et al. 2008), for every 1 h, while gradients were given for each 24 h.
- The uncertainties in the trends and variability estimates computed from GPS data are not well known, in particular regarding the impact of the cutoff angle. The choice of a cutoff angle is a trade-off between reducing stochastic or systematic errors. Ning et al. (2013) found a value of 25°, which was optimal when estimating linear IWV trends for 12 GPS site in Sweden and Finland. This value, however, cannot be applied directly to a global scale because of different site-related environments, different constellations of satellites, and different climates. Therefore, an elevation cutoff angle of 7°, which is also taken by many other IGS analysis centers, was used in our data processing.

Out of 794 sites, we selected 101 sites (see Fig. 1) that have data longer than 15 yr and converted the ZTD to the IWV. The procedure is summarized as follows:

The ZHD Z_h is first calculated (Davis et al. 1985):

$$Z_h = (2.2767 \pm 0.0015)\frac{P_0}{f(\lambda, H)} \tag{1}$$

and

$$f(\lambda, H) = [1 - 2.66 \times 10^{-3}\cos(2\lambda) - 2.8 \times 10^{-7}H], \tag{2}$$

where P_0 is the ground pressure; λ and H are the site latitude and the geoid height of the GPS site, respectively.

The ZWD Z_w is obtained by subtracting the ZHD from the estimated ZTD. Then the ZWD is converted to the IWV V by the parameter Q:

$$V = \frac{Z_w}{Q}, \tag{3}$$

where Q is calculated following the approach of Askne and Nordius (1987):

$$Q = 10^{-6}\rho_w R_w\left(\frac{k_3}{T_m} + k_2'\right), \tag{4}$$

where ρ_w is the density of liquid water; R_w is the specific gas constant of water vapor; and the values for the constants k_3 and k_2' were taken from Bevis et al. (1994).

For Eqs. (1) and (4), the ground pressure P_0 and the mean atmospheric temperature T_m were extracted from the reanalysis product of ECMWF (ERA-Interim), which is discussed in the next section.

b. ERA-Interim data

The ERA-Interim is the most recently developed reanalysis product by ECMWF (Simmons et al. 2006) that provides a temporal resolution of 6 h and a horizontal resolution of about 50 km. There is normally a difference between the model height and the GPS height. Thus, we carried out temporal, horizontal, and vertical interpolation of the ERA-Interim data to the time and position of the GPS site.

Details for the interpolation of the ECMWF data can be found in Heise et al. (2009) and are summarized as follows. For the horizontal interpolation, the ECMWF interpolation library (EMOSLIB; https://software.ecmwf.int/wiki/display/EMOS/What+is+EMOSLIB) was used. The 6-hourly ERA-Interim data were linearly interpolated to the temporal resolution of the GPS ZTD (1 h). The strategy used for the vertical interpolation depends on whether the GPS height is above or below the lowest ECMWF level. For the first case, the temperature and specific humidity of ECMWF were linearly interpolated, while pressure was logarithmically interpolated to the GPS height. For the latter case, the temperature was extrapolated using the mean temperature gradient of the three lowest ECMWF layers. The pressure was calculated by stepwise application of the barometric height formula for each 20 m, while the specific humidity was estimated in parallel, assuming that the mean relative humidity of the two lowest ECMWF levels was representative for the atmosphere below.

For reanalysis products, data acquired from many observing systems (i.e., numerous satellite instruments, radiosondes, buoys, and other components) were assimilated. Therefore, changes in the observing systems can result in mean shifts that interfere with true climate signals. Developments in the bias correction are thus required to ensure the best possible homogeneity of the reanalysis product. A key advantage of the ERA-Interim data is the variational bias correction system for satellite radiances developed at ECMWF (Dee and Uppala 2009), which allows the ERA-Interim product to proceed with minimized mean shifts.

The homogeneity of the ERA-Interim IWV time series was also validated by Bock et al. (2014) using a consistent long-term dataset of the IWV obtained from Doppler Orbitography Radiopositioning Integrated by Satellite (DORIS) measurements at 81 global sites. They found a good consistency between the IWV trends from the DORIS and ERA-Interim data. In addition, the ERA-Interim currently does not assimilate ground-based GPS-derived IWV data. Therefore, when comparing the GPS IWV data to the ERA-interim data, their changepoints are most likely different.

3. Methodology

a. *PMTred test*

A t test is normally used to determine if the mean values of two datasets are significantly different from each other. A t test is described as follows (X. Wang et al. 2007).

Let $V_t (t = 1, 2, 3, \ldots, N)$ denote an independent and identically distributed (IID) Gaussian series with a sample length of N. The detection of a potential changepoint in V_t is equivalent to test the null hypothesis

$$M_0: V_t \sim \mathcal{N}(\mu, \sigma^2) \tag{5}$$

against the alternative

$$M_a: \begin{cases} V_t \sim \mathcal{N}(\mu_1, \sigma^2), & t = 1, 2, 3, \ldots, k \\ V_t \sim \mathcal{N}(\mu_2, \sigma^2), & t = k+1, k+2, k+3, \ldots, N \end{cases}, \tag{6}$$

where V_t follows a normal distribution with a mean of μ and a variance of σ^2. When M_a is true while $\mu_1 \neq \mu_2$, the point at the time $t = k$ is defined as a changepoint. To locate the changepoint, we need to find out the most probable point that is associated with the maximal value of the following statistic:

$$T(k) = \frac{1}{\widehat{\sigma_k}} \left[\frac{k(N-k)}{N} \right]^{1/2} |\overline{V}_1 - \overline{V}_2|, \tag{7}$$

where

$$\widehat{\sigma_k^2} = \frac{1}{N-2} \left[\sum_{1 \le t \le k} (V_t - \overline{V}_1)^2 + \sum_{k+1 \le t \le N} (V_t - \overline{V}_2)^2 \right], \tag{8}$$

with

$$\overline{V}_1 = \frac{1}{k} \sum_{1 \le t \le k} V_t \tag{9}$$

and

$$\overline{V}_2 = \frac{1}{N-k} \sum_{k+1 \le t \le N} V_t. \tag{10}$$

Then the test statistic for locating the changepoint is given as:

$$T_{\max} = \max T(k). \tag{11}$$

X. Wang et al. (2007) proposed a penalized maximal t test (PMT) to empirically construct a penalty function that evens out the U-shaped false-alarm distribution over the relative position in the time series being tested. They modified Eq. (12) to

$$\mathrm{PT}_{\max} = \max P(k) T(k), \tag{12}$$

where $P(k)$ is the penalty function obtained empirically.

In addition, if there is a positive autocorrelation existing in the time series being tested and its effects are ignored, it is highly possible that wrong changepoints will be detected (Wang 2008). We calculated the autocorrelation of all time series that are going to be tested using the MATLAB command autocorr. The result showed significant lag-1 values (from 0.33 to 0.95) for most sites. Therefore, we decided to use the PMTred test that was proposed by Wang (2008).

To generate empirical critical values (CVs) for the PMTred test, we carried out a large number of Monte Carlo simulations for different sample length N. For each case, we simulated 1 000 000 homogenous IID Gaussian time series, $\mathcal{N}(0, 1)$, with a mean of zero and standard deviation of one. To take the lag-1 autocorrelation into account, we created the autocorrelated time series using a first-order autoregressive model (AR1). Because of limited computing time, simulations were only run for the monthly data with the sample length of 3 yr ($N = 36$ for a monthly data series), 5 yr ($N = 60$), 10 yr ($N = 120$), 15 yr ($N = 180$), 19 yr ($N = 228$), and 25 yr ($N = 300$). The CVs for other sample length were obtained by a linear interpolation of the simulated CVs. For each N, simulations were run for the lag-1 autocorrelation from 0 to 0.95 with an interval of 0.05. We saved values for the nominal significance level α for 10%, 5%, 1%, and 0.1% as CVs. The nominal significance level represents the chance at which the PMTred test mistakenly detects a changepoint in a homogenous time series. Therefore, $1 - \alpha$ (90%, 95%, 99%, and 99.9%) gives us the rate of the PMTred test correctly detecting a changepoint, which is often referred to as the level of confidence. A changepoint is detected when the PMTred test statistic PT_{max} is larger than the CV corresponding to a certain confidence level. Figure 2 depicts simulated CVs for different confidence levels and for different lag-1 autocorrelation as the function of the sample length N. It is clear that CVs are larger for an increasing autocorrelation and for a higher level of confidence.

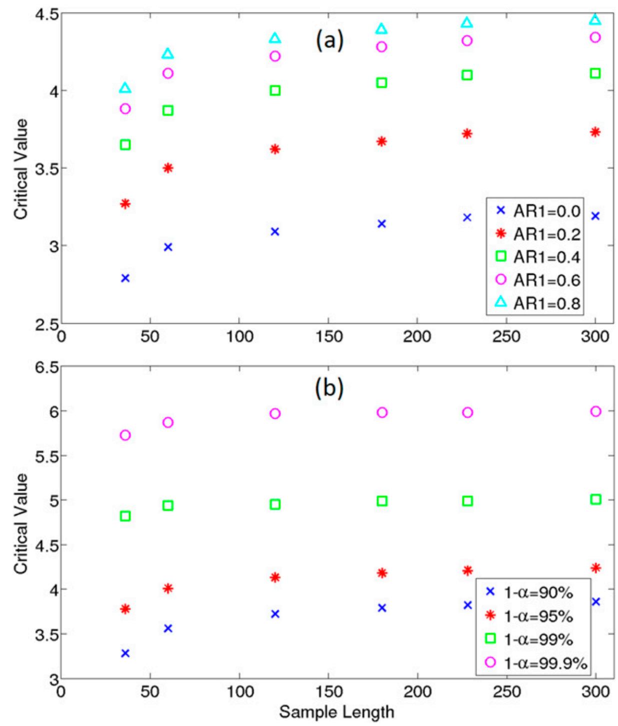

FIG. 2. Critical values (a) for five different lag-1 autocorrelation with a fixed confidence level ($1 - \alpha$) of 95% and (b) for four different confidence levels with a fixed lag-1 autocorrelation of 0.5, obtained from Monte Carlo simulations running for 1 000 000 times, as a function of the sample length N.

b. Changepoint detection and validation

For each selected GPS site, the time series of the monthly mean IWV difference between the GPS and ERA-Interim data was used for the PMTred test. This is because it requires too much computing time for the Monte Carlo simulation to obtain CVs for the daily data, which are also much noisier and for which it is more difficult, therefore, to correctly detect changepoints. Nevertheless, if it is required, the results obtained from the monthly data can be used to analyze and validate the results given by the daily data. One example of the time series of the monthly mean IWV and the difference between the GPS and ERA-Interim data for the site at Jozefoslaw (JOZE; 52.10°N, 21.03°E), Poland, is shown in Fig. 3, where both time series show a clear and consistent seasonal variation.

To have enough data to calculate the mean value, the PMTred test started (stopped) one year after (before) the beginning (end) of the time series. For example, if we have 19 yr of data, the monthly mean gives a total of 228 data points, and the PMTred test is only done on data points 13–215. If the test statistic PT_{max} is significant (larger than the CV), the point associated to PT_{max} is recorded as a potential changepoint. Thereafter, the time series is divided into two segments for further tests. This procedure is ongoing separately for each segment until the length of the segment reaches the minimum of 24 data points (less than 12 data points exist either before or after the point being tested).

The detection of a changepoint at an unknown (undocumented) location is different from finding one at a known (documented) location. The former case requires a larger CV than the latter one. For each IGS GPS site, there is a log file with a common format. The university or research institute that owns the GPS site is in charge of maintaining and updating the log file. All site-related changes (i.e., receiver, antenna, radome, and

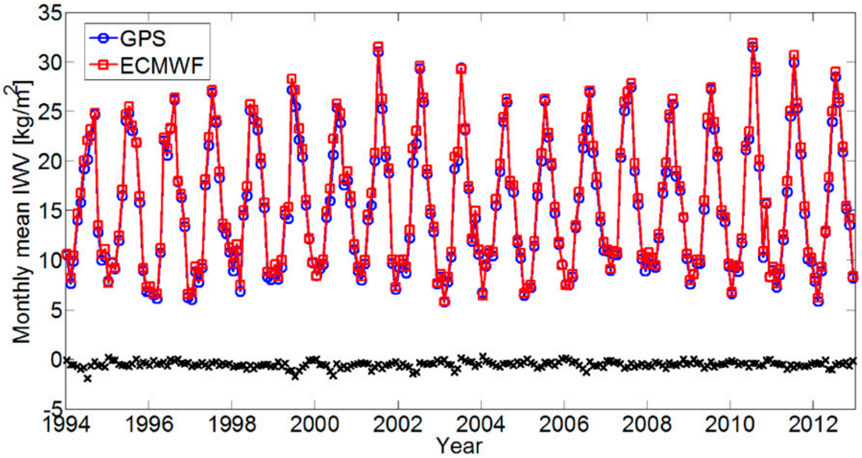

FIG. 3. The time series of the monthly mean IWV between the GPS and the ERA-Interim data for the GPS site at Jozefoslaw, Poland. The dark crosses are the IWV differences (GPS − ERA-Interim).

implementation of a microwave absorber) are specifically recorded in the log file. We first used the 95% confidence level as the CVs for the PMTred test to identify all potential changepoints. Thereafter, for each IGS site with detected changepoints, we searched a possible documented change for the time period of 6 months before and after the detected date in the log file. If such a documented change is found, the changepoint is recorded. Meanwhile, the detected date is changed to the corresponding documented date for future estimation of the mean shift. If no documented change is found or no log file exists (no IGS sites), the PT_{max} value of the changepoint is compared to the CV with a higher confidence level of 99.9%. If it is still significant (larger than the CV), the changepoint is also recorded. Figure 4 depicts the time series of monthly mean IWV difference for three sites (KIRU, GOLD, and SPT0). The mean shifts in the GPS IWV time series are due to the installation of the radome, the change of the antenna, and the implementation of the microwave absorber, respectively.

Although the variational bias correction was introduced in the ERA-Interim data, the reanalysis process is technically complex and must be constantly improved (Dee and Uppala 2009). Some biases might be left undetected and it is necessary to validate the ERA-Interim data using additional, independent sources of information. Therefore, in our study, further validation on all recorded changepoints is necessary in order to distinguish between the GPS-related changepoints and the ones in ERA-Interim. To this purpose, we estimated the resulting mean shift for each changepoint using different methods. The mean shift was first estimated using the IWV difference between the GPS and ERA-Interim data and, second, using the data from the neighboring GPS site. We first selected the potential site with the shortest distance while having the data at least one year before and after the date of the changepoint being validated. In addition, the same PMTred test was carried out on the data from the selected GPS site in order to ensure that there are no changepoints in the time period of interest (i.e., one year before and one year after the investigated date). Otherwise, the searching procedure will go on to the next neighboring GPS site. In addition, if there is a nearby site from very long baseline interferometry (VLBI), the mean shift was also estimated using the IWV difference between the GPS and VLBI data. The VLBI technique has the advantage of high long-term stability because of its stable instrumentation. Given this advantage, the VLBI-derived IWV can be used as a reference for detecting systematic errors in the IWV obtained from other techniques. If the mean shifts obtained from at least two methods have the same sign and the difference is less than the absolute value of the averaged mean shift over all methods, the changepoint is defined by a type set to G, meaning that it is GPS-related. If a significant shift is seen in the GPS − ERA-Interim method but not observed by other methods (GPS − GPS and/or GPS − VLBI), the type of the changepoint is assigned to E, meaning that the shift is due to the inconsistency in the ERA-Interim data. For the GPS sites with no nearby GPS and VLBI data or any other independent data available for validation, the type of the changepoint is set to 0, meaning that it is not possible to verify. Figure 5 gives one example of the G type of changepoint for the ONSA site. Three different methods were used in order to estimate the mean shift. The neighboring GPS site is SPT0, which is approximately 67 km from ONSA, and

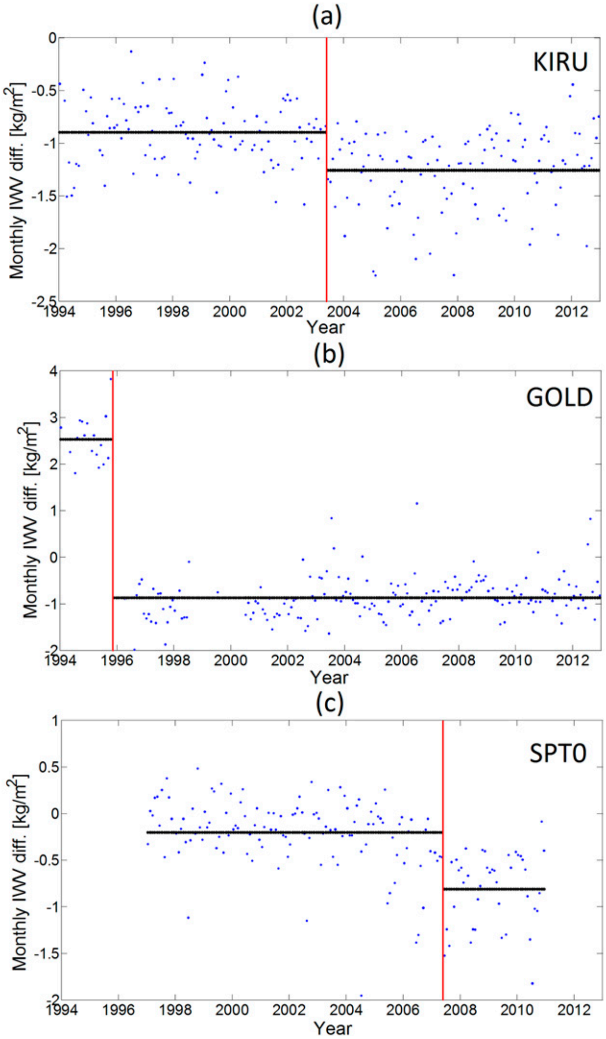

FIG. 4. Time series of the monthly mean IWV difference (GPS − ERA-Interim) for three GPS sites (a) KIRU (67.9°N, 21.1°E), (b) GOLD (35.4°N, 116.9°W), and (c) SPT0 (57.7°N, 12.9°E). Dark lines are the mean of IWV difference, and red lines indicate the date of the detected changepoints.

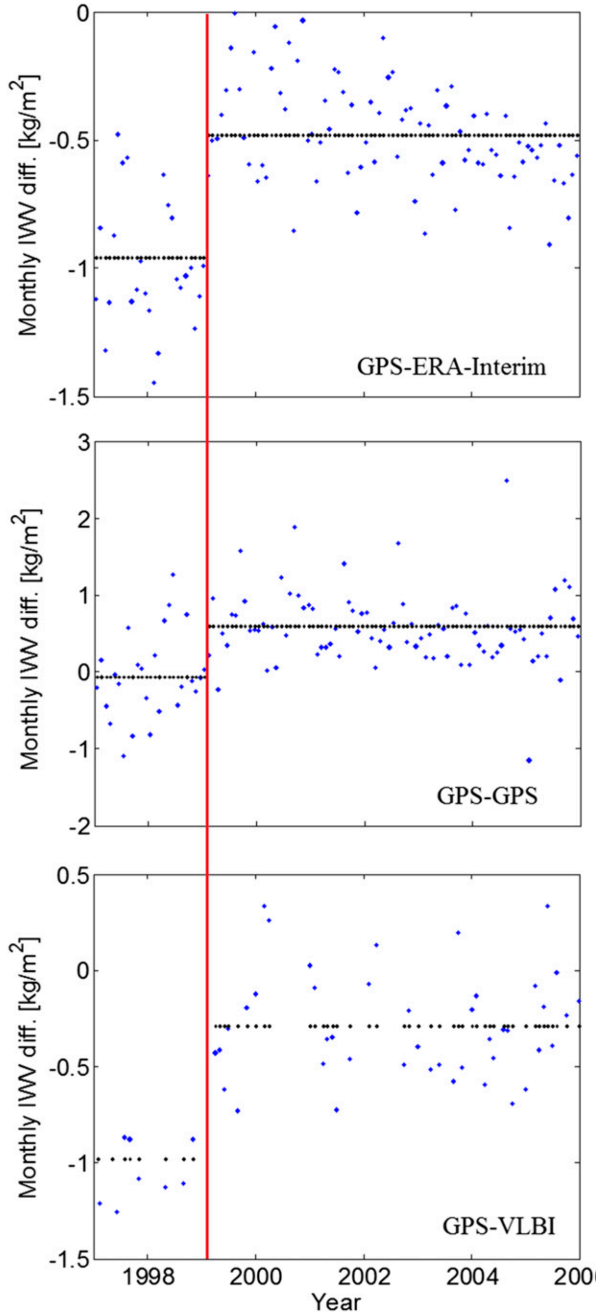

FIG. 5. Time series of the monthly mean IWV difference for the ONSA site (57.4°N, 11.9°E) given by three different methods: GPS − ERA-Interim, GPS − GPS, and GPS − VLBI. Dark lines are the mean of IWV difference, and the red line indicates the date of the detected changepoint.

the time period used for the estimation is from 1997 to 2006, where only one changepoint has been detected. The estimated mean shifts are −0.54, −0.69, and $-0.66\,\mathrm{kg\,m^{-2}}$ for GPS − ERA-Interim, GPS − GPS, and GPS − VLBI, respectively. The mean value of the three ($-0.63\,\mathrm{kg\,m^{-2}}$) was used for the correction of the GPS data for the ONSA site.

4. Results

a. Changepoints

All detected changepoints and corresponding mean shifts, estimated from different methods, are listed in Table 1, where the stations are ordered by the type of changepoint. Out of 101 GPS sites, the IWV difference time series for 47 sites were found containing changepoints.

Table 1 reveals that, in total, 62 changepoints were detected. After the validation, 45 of them were caused by the mean shifts in the GPS IWV time series, and 16

TABLE 1. Detected changepoints after applying the PMTred test to the monthly mean IWV difference time series between the GPS and ERA-Interim data. The PT_{max} is the test statistic, while the corresponding CV is given in the parenthesis. Type G means that the shift is due to the inconsistence in the GPS IWV time series and type E means that the shift is due to the inconsistence in the ECMWF IWV time series. Type 0 means that currently the shift is not able to be verified. Documented changes are given by the log files of the GPS sites.

Type	Site	Detected date	PT_{max} (CV)	Mean shift (GPS − ERA-Interim) ($kg\,m^{-2}$)	Mean shift (GPS − GPS) ($kg\,m^{-2}$)	Mean shift (GPS − VLBI) ($kg\,m^{-2}$)	Documented change
G	ONSA	Feb 1999	14.84 (4.30)	−0.54	−0.69	−0.66	1 Feb 1999 Radome change
G	KIRU	Jun 2003	8.57 (4.15)	0.34	0.42		12 Mar 2003 Radome installed
G	HOFN	Oct 2001	27.74 (4.40)	1.01	1.06		21 Sep 2001 Radome removed
G	WTZR	Jun 2009	8.57 (4.26)	−0.33	−0.15	−0.21	19 Jan 2009 Radome installed
G	SELE	Dec 2008	8.71 (4.40)	−0.99	−0.65		8 Jul 2008 Radome change
G	GOLD	Nov 1995	29.45 (4.40)	3.65	3.76		31 Oct 1995 Antenna change
G	FAIR	Jul 1996	13.26 (4.30)	−0.98		−0.93	16 Apr 1996 Radome installed
G	KELY	Sep 2001	52.72 (4.60)	3.01	3.69		14 Sep 2001 Radome removed
G	SPT0	Jun 2007	10.58 (4.21)	0.48	0.43	0.59	8 Jun 2007 Microwave absorber mounted
G	VNDP	Dec 1995	7.47 (4.15)	−0.65	−0.71		9 Nov 1995 Radome installed
G	TOW2	Oct 2002	6.45 (4.30)	−0.34	−0.20		1 Oct 2002 Antenna change
G	DUBO	Sep 1999	6.25 (4.41)	−0.38	−0.68		18 Aug 1999 Radome change
G	KERG	Feb 1999	7.88 (4.26)	0.38	0.20[a]		1 Apr 1999 Antenna change
G	KERG	Feb 2005	8.52 (6.32)	−0.27	−0.25[a]		
G	MATE	Dec 2001	8.10 (6.06)	0.39	0.17	0.20	
G	WES2	Jun 1998	7.93 (6.06)	−0.51	−0.36	−0.53	
G	VILL	Nov 2004	6.77 (5.94)	0.44	0.36		
G	SOFI	Jul 2009	8.19 (5.94)	−0.55	−0.76		
G	NYAL	Feb 2002	8.66 (6.09)	0.20	0.10	0.19	
G	POTS	Apr 1998	6.27 (6.26)	−0.26	−0.15		
G	POTS	Jul 2003	11.32 (6.10)	−0.11	−0.15		
G	URUM	Jun 2006	11.15 (6.23)	−1.23	−0.72	−1.39	
G	DARW	Jul 2000	6.13 (6.06)	−0.68	−0.48		
G	DARW	Jan 2006	6.57 (6.03)	1.05	0.58		
G	WILL	May 2005	6.57 (5.86)	−0.20	−0.39	−0.39	
G	VIMS	Apr 2008	9.48 (6.25)	−0.85	−0.93		
G	SYOG	Feb 2007	23.48 (6.26)	−0.59	−0.65		
G	SYOG	Jun 2009	7.37 (6.50)	−0.27	−0.41		
G	DNRC	Nov 2008	9.01 (6.14)	−0.58	−0.55		
G	MAW1	Sep 2007	11.63 (6.10)	−0.19	−0.19		
G	TIBB	Jun 1998	26.02 (6.29)	1.72	1.63		
G	TIBB	Jun 2003	7.65 (6.32)	0.29	0.12		
G	ZIMM	Nov 1996	6.98 (6.03)	0.35	0.29		
G	0194	Jun 2003	18.95 (6.23)	−0.89	−0.99		
G	FLIN	Sep 2000	9.60 (6.29)	−0.47	−0.56		
G	FLIN	Jul 2006	15.09 (6.25)	−0.27	−0.34		
G	FLIN	Jun 2011	7.92 (6.46)	−0.38	−0.39		
G	CAS1	Jun 2008	7.87 (6.14)	−0.22	−0.15		
G	COCO	Jul 2003	9.96 (6.14)	0.61	1.21		
G	BAKO	Sep 2008	10.43 (6.21)	1.72	2.17		

TABLE 1. (*Continued*)

Type	Site	Detected date	PT_{max} (CV)	Mean shift (GPS − ERA-Interim) ($kg\,m^{-2}$)	Mean shift (GPS − GPS) ($kg\,m^{-2}$)	Mean shift (GPS − VLBI) ($kg\,m^{-2}$)	Documented change
G	MAC1	Jan 1996	13.93 (6.21)	−0.54	−1.11		
G	BRMU	Jun 1997	7.72 (6.21)	−0.49	−0.47		
G	BRMU	Sep 2006	7.19 (6.23)	0.52	0.66		
G	DUBO	Nov 2007	10.09 (6.31)	−0.43	0.52		
G	IRKT	Oct 2002	9.00 (5.94)	−0.18	−0.20		
G	MATE	Dec 2001	8.10 (6.06)	0.39	0.17	0.20	
E	MAC1	Oct 2008	7.41 (6.22)	−0.11	0.05		
E	ANKR	Oct 2000	13.53 (6.21)	−0.92	0.02		
E	HOB2	May 2006	10.77 (6.10)	0.43	−0.03	0.01	
E	MAS1	Oct 2006	5.98 (5.86)	0.30	−0.03		
E	GODE	Jul 1998	9.37 (6.14)	−0.54	−0.07		
E	TIDB	Apr 1997	7.12 (6.14)	0.39	0.04		
E	POTS	Oct 2008	7.64 (6.11)	−0.33	−0.04		
E	SUWN	Dec 2003	7.74 (6.21)	−0.79	−0.08		
E	SHAO	Jul 2003	21.65 (6.26)	−1.26		0.09	
E	WUHN	Mar 1999	7.28 (6.32)	−0.48	0.06		
E	WUHN	Oct 2006	20.69 (6.26)	−1.51	−0.08		
E	BAKO	Sep 1999	7.62 (6.23)	−2.07	0.08		
E	PIE1	Jun 2007	6.31 (5.86)	−0.45	0.08	0.06	
E	CHUR	Sep 2008	6.22 (5.86)	−0.48	0.04		
E	VIMS	Apr 2000	8.61 (6.25)	−0.48	0.08		
E	LPGS	Aug 2006	9.12 (6.03)	0.45	−0.09		
0	KERG	Oct 2008	12.25 (4.32)	−0.36			28 Jul 2008 Antenna change

[a] The mean shift is given by GPS − DORIS.

were related to ERA-Interim. Because there are no neighboring GPS or VLBI data for the site KERG (49.4°S, 70.3°E), we used the data obtained from the collocated DORIS station (KERGUELEN) for the validation. The DORIS data were homogenized by Bock et al. (2014) for the time period from January 1993 to August 2008. Thus, we were able to validate the two changepoints detected in the years of 1997 and 2005 while the one in the year of 2008 was left unverified.

Fourteen G-type changepoints are supported by the documented changes where the PT_{max} varies from 6.25 to 52.72. Nine documented changes are radome related, because not all radomes are calibrated. One change resulted after the implementation of the microwave absorber, while five others are antenna related. For many old GNSS sites with long histories of observations, their antennas have not been individually calibrated. Therefore in our data processing, we used a standard IGS antenna PCV calibration for all sites. The standard IGS antenna PCV calibration provides a mean value of the calibrations from the same type of antennas. A position offset can result when the mean value is applied to the individual antenna, and the magnitude of the offset is station dependent. This was investigated by Baire et al. (2014), and they have shown that the offset in the vertical component can be as large as 10 mm, which approximately corresponds to a difference of 0.5 $kg\,m^{-2}$ in the IWV. We have carried out a similar investigation using one experimental GPS station located at Onsala Space Observatory (OSO) on the west coast of Sweden, where we processed data twice using two different antenna calibration models (IGS standard and individual calibration). The result reveals a mean offset around 0.4 $kg\,m^{-2}$ in the estimated IWV, which however shows very small variation (<0.05 $kg\,m^{-2}$) from day to day. This indicates that, if nothing else changed in the data processing, the shift due to different calibration models will be almost constant over the time.

There were thirty-two G-type changepoints not supported by the documentation where no hardware changes (i.e., antenna, radome, and microwave absorber) were recorded in the log file for the time period of 6 months before and after the detected. As discussed before, the data-processing-related changes (i.e., inconsistencies due to updates of the reference frame and applied models, implementation of a different elevation

TABLE 2. Differences in the estimated IWV trends before and after the bias corrections for the GPS sites with G-type changepoints (see Table 1). The sites are sorted by decreasing latitude.

GPS site	Lon (°E)	Lat (°N)	GPS trend before bias correction [kg (m^2 decade)$^{-1}$]	GPS trend after bias correction [kg (m^2 decade)$^{-1}$]	Difference [kg (m^2 decade)$^{-1}$]
NYAL	11.87	78.93	0.35 ± 0.19	0.46 ± 0.19	−0.11
SYOG	39.58	−69.01	0.39 ± 0.13	−0.31 ± 0.13	0.70
KIRU	20.97	67.86	0.16 ± 0.17	0.46 ± 0.17	−0.30
MAW1	62.87	−67.60	0.11 ± 0.15	−0.04 ± 0.15	0.15
KELY	−50.94	66.99	−1.28 ± 0.26	1.00 ± 0.24	−2.28
CAS1	110.52	−66.28	−0.01 ± 0.11	−0.14 ± 0.11	0.13
FAIR	−147.50	64.98	0.33 ± 0.22	0.09 ± 0.22	0.24
HOFN	−15.20	64.27	−0.79 ± 0.26	−0.03 ± 0.25	−0.76
SPT0	12.89	57.71	−0.41 ± 0.27	0.01 ± 0.27	−0.42
ONSA	11.93	57.40	0.79 ± 0.20	0.40 ± 0.20	0.39
FLIN	−101.98	54.73	0.95 ± 0.26	0.21 ± 0.26	0.74
MAC1	158.94	−54.50	0.71 ± 0.23	0.55 ± 0.23	0.16
POTS	13.07	52.38	0.67 ± 0.30	0.49 ± 0.30	0.18
WILL	−122.17	52.24	0.15 ± 0.18	−0.07 ± 0.18	0.22
IRKT	104.32	52.22	0.30 ± 0.25	0.14 ± 0.25	0.16
DUBO	−95.87	50.26	0.81 ± 0.30	0.91 ± 0.30	−0.10
WTZR	12.88	49.14	0.57 ± 0.27	0.44 ± 0.27	0.13
ZIMM	7.47	46.88	0.06 ± 0.17	0.18 ± 0.17	−0.12
URUM	87.60	43.81	0.41 ± 0.26	−0.41 ± 0.26	−0.82
SELE	77.02	43.18	0.43 ± 0.21	−0.22 ± 0.21	0.65
WES2	−71.49	42.61	0.87 ± 0.30	0.61 ± 0.30	0.26
SOFI	23.39	42.56	0.64 ± 0.24	0.19 ± 0.24	0.45
MATE	16.70	40.65	0.28 ± 0.19	0.47 ± 0.19	−0.19
VILL	−3.95	40.44	−0.31 ± 0.31	0.02 ± 0.31	−0.33
0194	139.55	39.19	1.30 ± 0.43	0.47 ± 0.43	0.83
DNRC	−75.52	39.16	1.28 ± 0.51	0.81 ± 0.51	0.47
TIBB	−122.45	37.89	−1.94 ± 0.35	−0.67 ± 0.34	−1.27
VIMS	−75.69	37.61	1.49 ± 0.52	0.86 ± 0.53	0.63
GOLD	−116.89	35.43	−0.90 ± 0.39	0.09 ± 0.39	−0.99
VNDP	−120.62	34.56	−0.08 ± 0.40	0.09 ± 0.40	−0.17
BRMU	−64.70	32.37	0.01 ± 0.30	0.20 ± 0.30	−0.19
TOW2	147.06	−19.27	0.58 ± 0.80	0.36 ± 0.80	0.22
DARW	131.13	−12.84	−0.66 ± 0.82	−0.21 ± 0.82	−0.45
COCO	96.83	−12.19	0.23 ± 0.79	1.03 ± 0.78	−0.80
BAKO	106.85	−6.49	−1.42 ± 0.60	0.24 ± 0.60	−1.66

cutoff angle, different mapping functions, and other differences in the processing strategies) have already been significantly reduced by homogenously reprocessed data. Therefore, those changepoints are most likely caused by the change of the electromagnetic environment (signal multipath). One example of such changes is given by the site SPT0, where an IWV bias around 0.5 kg m^{-2} is observed after the implementation of the microwave absorber onto the antenna of the site. The method discussed in this work can be applied to identify the multipath-related shifts that are stepwise. For the site where the multipath effects are not stepwise (e.g., because of growing vegetation and different soil moisture), identification of such changes is difficult, requiring careful and continuous documentation of the site. For example, if the cutting of trees has taken place in the area around the antenna, the time and the orientation of cutting (relative to the antenna) should be explicitly recorded. In addition, other methods are recommended in order to reduce the impact of such effect: that is, implementing microwave-absorbing material below the antenna plane (Ning et al. 2011) and/or using a higher elevation cutoff angle for the data processing (Ning and Elgered 2012).

One special case is seen for the changepoint detected in November 2007 for the site DUBO (50.3°N, 95.9°W). Both methods (GPS − ERA-Interim and GPS − GPS) give significant mean shifts (−0.43 and 0.52 kg m^{-2}, respectively), but with different sign. This indicates that shifts exist both in the GPS and ERA-Interim IWV time series.

b. Comparison of IWV trends

Linear IWV trends were estimated for all 101 GPS sites using a model that considers the annual and the semiannual variations in the IWV (Ning and Elgered 2012). For each GPS-related changepoint (G type), the mean shifts estimated from the different methods were

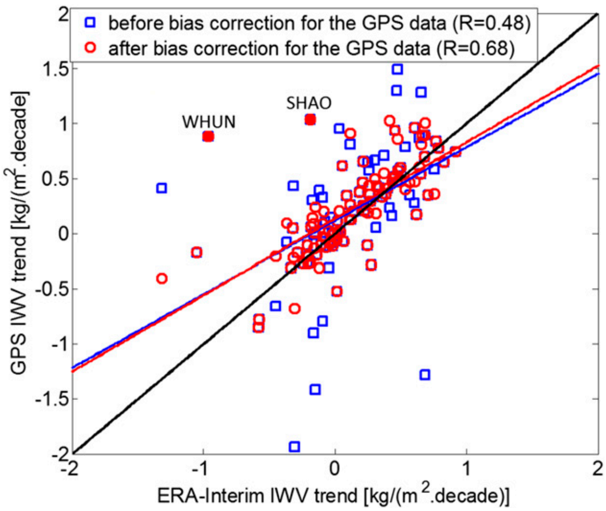

FIG. 6. Correlations between the IWV trends, estimated for 101 sites from the ERA-Interim and the GPS data before and after the corrections for the mean shifts for 35 sites. The trends estimated for the two sites, WUHN and SHAO, are indicated by solid symbols. The blue and red lines are the linear fits of the plotted data, while the black line indicates the perfect correlation.

averaged, and the resulting value was applied for the GPS data correction. This was done by adding the mean shift to all IWV before the date of the changepoint. The data from the site KERG were not homogenized because one changepoint was unable to be validated. Table 2 shows the estimated linear trends that are in the range from -1.94 to $+1.49$ kg (m^2 decade)$^{-1}$ when no bias corrections were implemented. After the corrections, the variation of the trends becomes smaller [from -0.67 to $+1.03$ kg (m^2 decade)$^{-1}$]. Depending on the magnitude of the mean shift and the location of the changepoint, the trend difference varies from -2.28 to 0.83 kg (m^2 decade)$^{-1}$. In addition, we calculated the uncertainties of the linear trends, which were rescaled in order to be consistent with the misfit of the model as described in Nilsson and Elgered (2008) and are in the range 0.11–0.82 kg (m^2 decade)$^{-1}$. Largest values are observed at latitudes lower than -20°N. We note that there is almost no difference seen in the trend uncertainties after the bias corrections. This is because the uncertainty is mostly caused by the natural short-term variability in the water vapor content. Table 2 also shows that for the most of sites the uncertainties are comparable to the values of the trend, indicating that the length of the GPS time series is still too short to search for climate change. Nevertheless, the obtained trends can be compared to the trends obtained using other methods for validation purpose (e.g., radiosondes, water vapor radiometers, and/or climate models).

Figure 6 depicts the IWV trends estimated from the GPS data before and after the bias correction, together with the trends obtained from the ERA-Interim data (no bias correction implemented). The correlation between the trends is improved from 0.48 to 0.68 after using the corrected GPS data. Figure 6 also reveals a clear difference for two sites, WUHN and SHAO (31.1°N, 121.2°E), on the east part of China, where significant positive trends are seen for the GPS data while the ERA-Interim data give negative trends. A similar difference was found by Bock et al. (2014) in the same area between the IWV trends obtained from the DORIS data (positive trends) and from the ERA-Interim data (negative trends). The consistent trends between the DORIS and the GPS data indicate that the detected changepoints for the two sites are most likely related to the ERA-Interim data.

The GPS IWV were also compared to the IWV obtained from a globally homogenized radiosonde dataset where the radiosonde humidity records were homogenized using two statistical tests in order to remove mean shifts due to cold and dry mean shifts as well as sensor changes (Dai et al. 2011). The maximum distance between the pair of the GPS and radiosonde sites is 100 km, while the threshold for the height difference is 100 m. Globally we found 47 paired sites where 18 of the GPS sites contain changepoints. Figure 7 depicts the time series of the monthly IWV anomaly obtained from the homogenized and nonhomogenized GPS data together with the ones given by the nearby radiosonde data. An improved agreement is seen for all three sites after using the homogenized GPS data. In addition, we compared the GPS-derived IWV trends to the trends obtained from the radiosonde data. To reduce the impact on the estimated IWV trends due to data gaps, the comparisons were made by selecting the time epochs where the two techniques have simultaneous data. Figure 8 depicts correlations of the IWV trends where the correlation coefficient improves significantly from 0.32 to 0.44 after the correction for the mean shift implemented in the GPS data.

5. Conclusions

The possible temporal shifts in the long time series of the IWV, obtained from the reprocessed data acquired from 101 GPS sites, were comprehensively investigated. The data were tested by the penalized maximal *t* test modified to account for first-order autoregressive noise in time series (PMTred) in order to identify potential changepoints.

We used the time series of the monthly mean IWV difference between the GPS data and the ECMWF

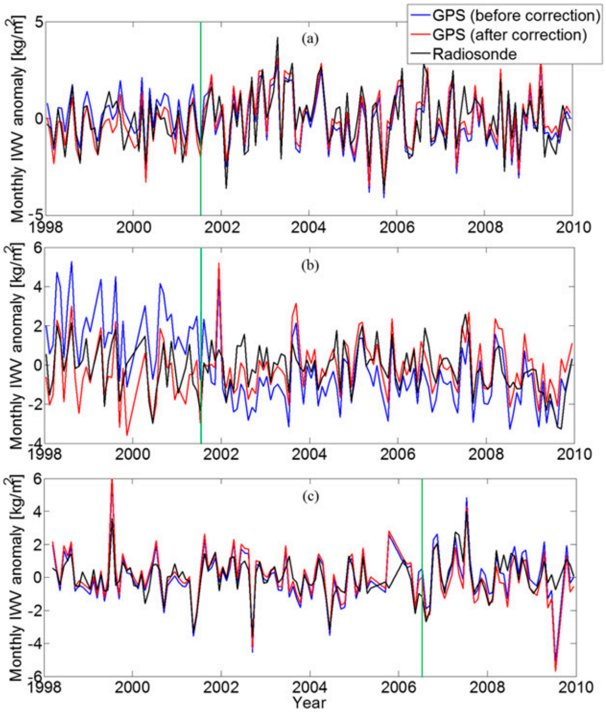

FIG. 7. Time series of the monthly IWV anomaly for three GPS sites: (a) HOFN (64.3°N, −15.2°E), (b) KELY (67.0°N, −50.9°E), and (c) URUM (43.8°N, 87.6°E). Dark lines are the anomaly obtained from radiosonde data; blue and red lines are the ones obtained from the GPS data before and after the correction of the mean shifts, respectively. Green lines indicate the date of the detected changepoint.

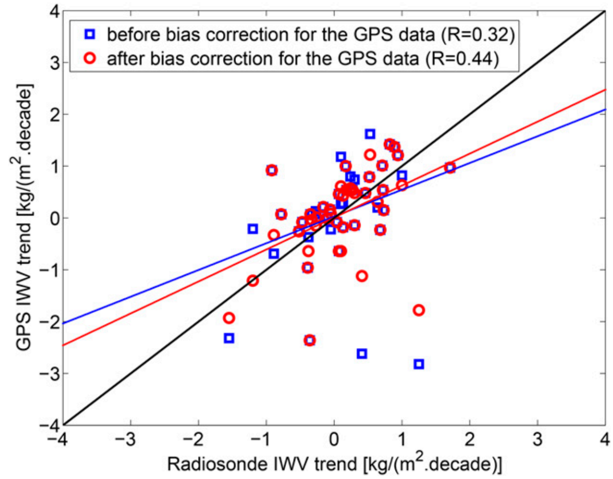

FIG. 8. Correlations between the IWV trends, estimated for 47 sites, from the radiosonde and the GPS data before and after the shift corrections for 18 GPS sites. The blue and red lines are the linear fits of the plotted data, while the black line indicates the perfect correlation.

reanalysis data (ERA-Interim) for the PMTred test. The result shows that 47 out of 101 sites were found containing, in total, 62 changepoints. For the validation purpose, the resulting mean shifts of the detected changepoints given by GPS − ERA-Interim were compared with the ones calculated using independent data sources [i.e., data obtained from nearby GPS and/or VLBI sites (the DORIS data were used for one site)]. The result indicates that 45 detected changepoints were due to the inconsistences in the GPS IWV time series, and 16 were related to ERA-Interim, while one point cannot be verified because of missing validation data.

All GPS IWV time series with validated changepoints were homogenized by applying a mean shift that was estimated from different methods (GPS − ERA-Interim, GPS − GPS, and GPS − VLBI). A better agreement is seen between the IWV trends obtained from the homogenized GPS data and the ones given by the ERA-Interim data.

The GPS-derived IWV trends for 47 sites, where 18 of them contain changepoints, were also compared to the corresponding trends obtained from nearby homogenized radiosonde data. After the bias correction for the GPS data, the correlation coefficient of the trends is improved by 38%.

For each GPS site, the detected and validated changepoints in this work can be used to compare with the results from other data processing. However, the calculated mean shift cannot be directly applied if others used different data processing strategies, i.e., elevation cutoff angles, antenna models, and software. Future studies are recommended in order to investigate the sensitivity of the detected changepoints to the above factors.

The method presented in this work is not only used for the homogenization of the GNSS data but also for identifying temporal mean shifts in the ERA-Interim. Two changepoints, detected for two sites—SHAO and WUHN—are most likely to be related to the ERA-Interim data.

In the future, the PMTred test will be carried out for all TIGA reprocessed GPS data. All detected changepoints will be validated in the same manner as presented in this work. The date of the validated changepoints will be recorded in a table together with the correspondingly resulting mean shifts (estimated from independent methods). Such tables and the homogenized GPS IWV dataset will be openly accessible for other research communities.

Acknowledgments. The authors thank Junhong Wang for providing the homogenized radiosonde dataset. We are also grateful to Cuixian Lu and Xinxin Li for providing the VLBI data set. We thank the IGS and the SONEL data center (www.sonel.org) for providing

GNSS observation data and Olivier Bock for providing DORIS data for the site KERG. The maps were produced using the Generic Mapping Tools (GMT) Wessel and Smith (1998).

REFERENCES

Askne, J., and H. Nordius, 1987: Estimation of tropospheric delay for microwaves from surface weather data. *Radio Sci.*, **22**, 379–386, doi:10.1029/RS022i003p00379.

Baire, Q., C. Bruyninx, J. Legrand, E. Pottiaux, W. Aerts, P. Defraigne, N. Bergeot, and J. M. Chevalier, 2014: Influence of different GPS receiver antenna calibration models on geodetic positioning. *GPS Solutions*, **18**, 529–539, doi:10.1007/s10291-013-0349-1.

Bengtsson, L., 2010: The global atmospheric water cycle. *Environ. Res. Lett.*, **5**, 025202, doi:10.1088/1748-9326/5/2/025202.

Bevis, M., S. Chiswell, T. A. Herring, R. A. Anthes, C. Rocken, and R. H. Ware, 1994: GPS meteorology: Mapping zenith wet delays onto precipitable water. *J. Appl. Meteor.*, **33**, 379–386, doi:10.1175/1520-0450(1994)033<0379:GMMZWD>2.0.CO;2.

Bock, O., P. Willis, J. Wang, and C. Mears, 2014: A high-quality, homogenized, global, long-term (1993–2008) DORIS precipitable water data set for climate monitoring and model verification. *J. Geophys. Res.*, **119**, 7209–7230, doi:10.1002/2013JD021124.

Böhm, J., J. Kouba, and H. Schuh, 2008: Forecast Vienna Mapping Functions 1 for real-time analysis of space geodetic observations. *J. Geod.*, **83**, 397–401, doi:10.1007/s00190-008-0216-y.

Buehler, S. A., A. von Engeln, E. Brocard, V. O. John, T. Kuhn, and P. Eriksson, 2006: Recent developments in the line-by-line modeling of outgoing longwave radiation. *J. Quant. Spectrosc. Radiat. Transfer*, **98**, 446–457, doi:10.1016/j.jqsrt.2005.11.001.

Dai, A., J. Wang, P. W. Thorne, D. E. Parker, L. Haimberger, and X. L. Wang, 2011: A new approach to homogenize daily radiosonde humidity data. *J. Climate*, **24**, 965–991, doi:10.1175/2010JCLI3816.1.

Davis, J. L., T. A. Herring, I. I. Shapiro, A. E. E. Rogers, and G. Elgered, 1985: Geodesy by radio interferometry: Effects of atmospheric modelling errors on estimates of baseline length, *Radio Sci.*, **20**, 1593–1607, doi:10.1029/RS020i006p01593.

Dee, D. P., and S. Uppala, 2009: Variational bias correction of satellite radiance data in the ERA-Interim reanalysis. *Quart. J. Roy. Meteor. Soc.*, **135**, 1830–1841, doi:10.1002/qj.493.

Deng, Z., 2012: GPS meteorology with signal frequency receivers. Deutsches GeoForschungsZentrum Tech. Rep. STR12/09, 110 pp., doi:10.2312/GFZ.b103-12099.

——, G. Gendt, and T. Schöne, 2016: Status of the IGS-TIGA tide gauge data reprocessing at GFZ. International Association of Geodesy Symposia, doi:10.1007/1345_2015_156, in press.

Gradinarsky, L. P., J. Johansson, H. R. Bouma, H.-G. Scherneck, and G. Elgered, 2002: Climate monitoring using GPS. *Phys. Chem. Earth*, **27**, 335–340, doi:10.1016/S1474-7065(02)00009-8.

Heise, S., G. Dick, G. Gendt, T. Schmidt, and J. Wickert, 2009: Integrated water vapor from IGS ground-based GPS observations: Initial results from a 5-min data set. *Ann. Geophys.*, **27**, 2851–2859, doi:10.5194/angeo-27-2851-2009.

Johansson, J. M., 1998: GPS antenna and site effects. *Advances in Positioning and Reference Frames*, F. Brunner, Ed., International Association of Geodesy Symposia, Vol. 118, Springer, 229–235, doi:10.1007/978-3-662-03714-0_37.

Larson, K. M., J. J. Braun, E. E. Small, V. U. Zavorotny, E. D. Gutmann, and A. L. Bilich, 2010: GPS multipath and its relation to near-surface soil moisture content. *IEEE J. Sel. Top. Appl. Earth Obs. Remote Sens.*, **3**, 91–99, doi:10.1109/JSTARS.2009.2033612.

Lyard, F., F. Lefevre, T. Letellier, and O. Francis, 2006: Modelling the global ocean tides: Modern insights from FES2004. *Ocean Dyn.*, **56**, 394–415, doi:10.1007/s10236-006-0086-x.

Nilsson, T., and G. Elgered, 2008: Long-term trends in the atmospheric water vapor content estimated from ground-based GPS data. *J. Geophys. Res.*, **113**, D19101, doi:10.1029/2008JD010110.

Ning, T., and G. Elgered, 2012: Trends in the atmospheric water vapor content from ground-based GPS: The impact of the elevation cutoff angle. *IEEE J. Sel. Top. Appl. Earth Obs. Remote Sens.*, **5**, 744–751, doi:10.1109/JSTARS.2012.2191392.

——, ——, and J. M. Johansson, 2011: The impact of microwave absorber and radome geometries on GNSS measurements of station coordinates and atmospheric water vapour. *Adv. Space Res.*, **47**, 186–196, doi:10.1016/j.asr.2010.06.023.

——, ——, U. Willén, and J. M. Johansson, 2013: Evaluation of the atmospheric water vapor content in a regional climate model using ground-based GPS measurements. *J. Geophys. Res.*, **118**, 329–339, doi:10.1029/2012JD018053.

Pierdicca, N., L. Guerriero, R. Giusto, M. Broioni, and A. Egido, 2014: SAVERS: A simulator of GNSS reflections from bare and vegetated soils. *IEEE Trans. Geosci. Remote Sens.*, **52**, 6542–6554, doi:10.1109/TGRS.2013.2297572.

Saastamoinen, J., 1973: Contributions to the theory of atmospheric refraction. *Bull. Geod.*, **107**, 13–34, doi:10.1007/BF02522083.

Schmid, R., P. Steigenberger, G. Gendt, M. Ge, and M. Rothacher, 2007: Generation of a consistent absolute phase center correction model for GPS receiver and satellite antennas. *J. Geod.*, **81**, 781–798, doi:10.1007/s00190-007-0148-y.

Schöne, T., N. Schön, and D. Thaller, 2009: IGS Tide Gauge Benchmark Monitoring Pilot Project (TIGA): Scientific benefits. *J. Geod.*, **83**, 249–261, doi:10.1007/s00190-008-0269-y.

Seidel, D. J., and Coauthors, 2009: Reference upper-air observations for climate: Rationale, progress, and plans. *Bull. Amer. Meteor. Soc.*, **90**, 361–369, doi:10.1175/2008BAMS2540.1.

Simmons, A., S. Uppala, D. Dee, and S. Kobayashi, 2006: ERA-Interim: New ECMWF reanalysis products from 1989 onwards. *ECMWF Newsletter*, No. 110, ECMWF, Reading, United Kingdom, 25–35.

Steigenberger, P., V. Tesmer, M. Krügel, D. Thaller, R. Schmid, S. Vey, and M. Rothacher, 2007: Comparisons of homogeneously reprocessed GPS and VLBI long time-series of troposphere zenith delays and gradients. *J. Geod.*, **81**, 503–514, doi:10.1007/s00190-006-0124-y.

Teunissen, P. J. G., 1995: The least-squares ambiguity decorrelation adjustment: A method for fast GPS integer ambiguity estimation. *J. Geod.*, **70**, 65–82, doi:10.1007/BF00863419.

Trenberth, K. E., A. Dai, R. M. Rasmussen, and D. B. Parsons, 2003: The changing character of precipitation. *Bull. Amer. Meteor. Soc.*, **84**, 1205–1217, doi:10.1175/BAMS-84-9-1205.

Vey, S., R. Dietrich, M. Fritsche, A. Rülke, P. Steigenberger, and M. Rothacher, 2009: On the homogeneity and interpretation of precipitable water time series derived from global GPS observations. *J. Geophys. Res.*, **114**, D10101, doi:10.1029/2008JD010415.

——, ——, A. Rülke, M. Fritsche, P. Steigenberger, and M. Rothacher, 2010: Validation of precipitable water vapor within the NCEP/DOE Reanalysis using global GPS observations from one decade. *J. Climate*, **23**, 1675–1695, doi:10.1175/2009JCLI2787.1.

Wang, J., L. Zhang, A. Dai, T. V. Hove, and J. V. Baelen, 2007: A near-global, 2-hourly data set of atmospheric precipitable water from ground-based GPS measurements. *J. Geophys. Res.*, **112**, D1107, doi:10.1029/2006JD007529.

Wang, X. L., 2008: Accounting for autocorrelation in detecting mean shifts in climate data series using the penalized maximal *t* or *F* test. *J. Appl. Meteor. Climatol.*, **47**, 2423–2444, doi:10.1175/2008JAMC1741.1.

——, Q. H. Wen, and Y. Wu, 2007: Penalized maximal *t* test for detecting undocumented mean change in climate data series. *J. Appl. Meteor.*, **46**, 916–931, doi:10.1175/JAM2504.1.

Wessel, P., and W. H. F. Smith, 1998: New, improved version of generic mapping tools released. *Eos, Trans. Amer. Geophys. Union*, **79**, 579, doi:10.1029/98EO00426.